

Angled sidewalls in silicon slot waveguides: conformal filling and mode properties

A. Säynätjoki^{1*}, T. Alasaarela¹, A. Khanna¹, L. Karvonen¹,
P. Stenberg², M. Kuittinen², A. Tervonen¹ and S. Honkanen¹

¹Department of Micro and Nanosciences, Helsinki University of Technology (TKK);
Micronova, Tietotie 3, FIN-02015 Espoo, FINLAND

²Department of Physics, University of Joensuu, FINLAND

antti.saynatjoki@tkk.fi

Abstract: Effect of angled sidewalls on the filling and properties of silicon slot waveguides is discussed. We demonstrate complete filling of slot waveguide structures with oxide material systems using the atomic layer deposition technique and discuss use of various slot filling materials. Properties of the optical modes in angled-sidewall slot waveguides are studied. Enhanced vertical confinement is obtained with certain waveguide parameters. The reduced effective mode area enhances e.g. nonlinear effects in the waveguide. We discuss the use of atomic layer deposition in realization of filled slot waveguides optimized for all-optical functionalities.

© 2009 Optical Society of America

OCIS codes: OCIS codes: (130.2790) Guided waves; (130.3130) Integrated optics materials; (230.7370) Waveguides; (230.7390) Waveguides, planar; (250.5300) Photonic Integrated Circuits.

References and links

1. M. Lipson, "Guiding, modulating, and emitting light on silicon - challenges and opportunities," *J. Lightwave Technol.* **23**, 4222 (2005).
2. G. T. Reed, "The optical age of silicon," *Nature* **427**, 595 (2004).
3. T. Tsuchizawa, K. Yamada, H. Fukuda, T. Watanabe, J. Takahashi, M. Takahashi, T. Shoji, E. Tamechika, S. Itabashi, and H. Morita, "Microphotonics devices based on silicon microfabrication technology," *IEEE J. Sel. Top. Quantum Electron.* **11**, 232 (2005).
4. S. Afshar V. and T. M. Monro, "A full vectorial model for pulse propagation in emerging waveguides with subwavelength structures part I: Kerr nonlinearity," *Opt. Express* **17**, 2298-2318 (2009).
5. Q. Xu, V.R. Almeida, R.R. Panepucci, and M. Lipson, "Experimental demonstration of guiding and confining light in nanometer-size low-refractive-index material," *Opt. Lett.* **29**, 1626 (2004).
6. Rong Sun, Po Dong, Ning-ning Feng, Ching-yin Hong, Jurgen Michel, Michal Lipson, and Lionel Kimerling, "Horizontal single and multiple slot waveguides: optical transmission at $\lambda=1550$ nm," *Opt. Express* **15**, 17967-17972 (2007).
7. N. Daldosso and L. Pavesi, "Nanosilicon photonics", *Laser & Photon. Rev.*, 1-27 (2009).
8. N.-N. Feng, R. Sun, L. C. Kimerling, and J. Michel, "Lossless strip-to-slot waveguide transformer," *Opt. Lett.* **32**, 1250-1252 (2007).
9. G. Wang, T. Baehr-Jones, M. Hochberg, and A. Scherer, "Design and fabrication of segmented, slotted waveguides for electro-optic modulation", *Appl. Phys. Lett.* **91**, 143109 (2007).
10. E. Jordana, J.M. Fedeli, P. Lyan, J.P. Colonna, P.E. Gautier, N. Daldosso, L. Pavesi, Y. Lebour, P. Pellegrino, B. Garrido, J. Blasco, T. Cuesta-Soto, P. Sanchis, "Deep-UV Lithography Fabrication of Slot Waveguides and Sandwiched Waveguides for Nonlinear Applications," *Group IV Photonics, 2007 4th IEEE International Conference on paper ThC3*.
11. T. Baehr-Jones, M. Hochberg, C. Walker, and A. Scherer, "High-Q optical resonators in silicon-on-insulator-based slot waveguides," *Appl. Phys. Lett.* **86**, 081101 (2005).

12. R.L. Puurunen, "Surface chemistry of atomic layer deposition: A case study for the trimethylaluminum/water process," *J. Appl. Phys.* **97**, 121301 (2005).
13. T. Pilvi, E. Puukilainen, U. Kreissig, M. Leskelä, M. Ritala, "Atomic Layer Deposition of MgF₂ Thin Films Using TaF₅ as a Novel Fluorine Source", *Chem. Mater.* **20**, 5023-5028 (2008).
14. P. Müllner, R. Hainberger, "Optical characteristics of V-groove waveguide structures," *Proc. SPIE* **7220**, 722004 (2009).
15. P. Sanchis, J. Blasco, A. Martinez, J. Marti, "Design of Silicon-Based Slot Waveguide Configurations for Optimum Nonlinear Performance," *J. Lightwave Technol.* **25**, 1298-1305 (2007).
16. F. Dell'Olio and V. M. Passaro, "Optical sensing by optimized silicon slot waveguides," *Opt. Express* **15**, 4977-4993 (2007).
17. A. Säynätjoki, L. Karvonen, A. Khanna, T. Alasaarela, A. Tervonen, S. Honkanen, "Silicon slot waveguides for nonlinear optics," *Proc. SPIE* **7212**, 72120T (2009).
18. R. Adair, L.L. Chase, and S.A. Payne, "Nonlinear refractive index of optical crystals," *Phys. Rev. B* **39**, 3337 - 3350 (1989).
19. T. Alasaarela, A. Säynätjoki, T. Hakkarainen, S. Honkanen, "Feature size reduction of silicon slot waveguides by partial filling using atomic layer deposition", *Opt. Eng.* **48**, 080502 (2009).
20. C. Koos, L. Jacome, C. Poulton, J. Leuthold, and W. Freude, "Nonlinear silicon-on-insulator waveguides for all-optical signal processing," *Opt. Express* **15**, 5976-5990 (2007).
21. C. Koos, P. Vorreau, T. Vallaitis, P. Dumon, W. Bogaerts, R. Baets, B. Esembeson, I. Biaggio, T. Michinobu, F. Diederich, W. Freude and J. Leuthold, "All-optical high-speed signal processing with silicon-organic hybrid slot waveguides," *Nat. Photonics* **3**, 216-219 (2009).
22. B. Esembeson, M. L. Scimeca, T. Michinobu, F. Diederich, I. Biaggio, "A high-optical quality supramolecular assembly for third-order integrated nonlinear optics," *Adv. Mater.* **20**, 4584-4587 (2008).
23. S. Morino, T. Yamashita, K. Horie, T. Wada, H. Sasabe, "Third-order nonlinear optical properties of aromatic polyisoimides", *Reactive and Functional Polymers* **44**, 183-188 (2000).
24. M. Putkonen, J. Harjuoja, T. Sajavaara and L. Niinistö, "Atomic layer deposition of polyimide thin films", *J. Mater. Chem.*, **17**, 664 - 669 (2007).
25. Y. Guo, K. S. Chiang, H. Li, *Nonlinear photonics*, (Springer).
26. M. E. Lines, "Influence of d orbitals on the nonlinear optical response of transparent transition-metal oxides," *Phys. Rev. B.* **43**, 11978-11990 (1991).
27. A. Major, F. Yoshino, I. Nikolakakos, J. Stewart Aitchison, and P. W. E. Smith, "Dispersion of the nonlinear refractive index in sapphire," *Opt. Lett.* **29**, 602-604 (2004).
28. R. Spano, N. Daldosso, M. Cazzanelli, L. Ferraioli, L. Tartara, J. Yu, V. Degiorgio, E. Jordana, J. M. Fedeli, and L. Pavesi, "Bound electronic and free carrier nonlinearities in Silicon nanocrystals at 1550nm", *Opt. Express* **17**, 3941-3950 (2009).
29. FimmWave 5.1, November 2008, PhotonDesign Ltd.; www.photond.com.
30. A. Gondarenko, S. Preble, J. Robinson, L. Chen, H. Lipson, and M. Lipson, "Spontaneous Emergence of Periodic Patterns in a Biologically Inspired Simulation of Photonic Structures," *Phys. Rev. Lett.* **96**, 143904 (2006).
31. K. Worhoff, J. D. B. Bradley, F. Ay, D. Geskus, T. P. Blauwendraat, M. Pollnau, "Reliable Low-Cost Fabrication of Low-Loss Al₂O₃:Er³⁺ Waveguides With 5.4-dB Optical Gain," *IEEE J. Quantum Electron.* **45**, 454-461 (2009).
32. M. Tiitta, L. Niinistö, "Volatile Metal beta-Diketonates: ALE and CVD precursors for electroluminescent device thin films," *Chem. Vap. Deposition* **3**, 167-182 (1997).
33. Jacob T. Robinson, Kyle Preston, Oskar Painter, and Michal Lipson, "First-principle derivation of gain in high-index-contrast waveguides," *Opt. Express* **16**, 16659-16669 (2008).

1. Introduction

The high refractive index and mature processing technology of silicon enable integrated optical devices with sub-micron sized features. In a tightly confined optical field, nonlinear effects can be invoked at moderate power levels, enabling all-optical silicon devices such as a Raman laser, a wavelength converter, a signal regenerator and logic gates [1–3]. A thorough, general full-vectorial study on the Kerr nonlinearity in nanowaveguides has been carried out in [4]. Light can be confined into a nanoscale low-index slot on silicon, which yields even stronger lateral confinement than the conventional silicon-on-insulator (SOI) based strip waveguide [5]. Using the slot waveguide structure, silicon-based waveguides can also be efficiently integrated with optimal non-linear materials (e.g. highly nonlinear materials with low two-photon absorption), or materials for other purposes (e.g. light emission). Therefore, slot waveguides may enhance not only the performance of silicon photonic chips, but also add new functionalities into them.

There are two principally different approaches in manufacturing silicon slot waveguides. One can grow a three-layer stack, where the low-index material is sandwiched between two layers of silicon. The slot width is not limited by the lithography, and with an optimized growth process the slot interfaces can be made very smooth. Therefore, propagation loss as low as 4 dB/cm has been achieved using such a horizontal slot waveguide [10]. However, the top silicon layer typically needs to be grown and it is therefore amorphous or polycrystalline silicon, whose optical and electrical properties are compromised compared to single-crystalline silicon.

One can also make the slot waveguide by etching two silicon rails into an SOI substrate. The fabrication of such a vertical slot waveguide is therefore very compatible to fabrication of silicon strip waveguides; only one patterning step and one growth step are needed to make such a vertical slot waveguide with a desired filling material. One can also realize efficient couplers between vertical slot waveguides and strip waveguides just by pattern definition [8], and the vertical slot waveguide enables even more complex structures for e.g. efficient electrical injection [9]. Moreover, the silicon in the structure will be entirely single-crystalline, therefore no compromises in electrical or optical properties are needed. However, complete filling of the narrow slots has proved to be a difficult task [10], and voids inside the waveguide may cause detrimental amounts of scattering loss. Due to the high demands in lithography and overgrowth, the lowest losses reported for vertical slot waveguides are in the order of 10 dB/cm (e.g. [11]).

Atomic layer deposition (ALD) is a growth technique that provides extremely conformal, voidless films with an excellent thickness accuracy and step coverage even with high aspect-ratio structures. Therefore, ALD is a very promising method for filling photonic structures. Considering silicon photonics in particular, ALD has proved its CMOS compatibility, as chip manufacturers have taken ALD grown hafnium oxide into production as a high- k gate oxide material. ALD growth has been applied for a wide range of materials [12, 13].

The etching processes used in the manufacturing of silicon photonics typically produce angled sidewalls, which affects some properties of the slot waveguide. The angled sidewalls provide improved accessibility from top, which has been proposed to be used in sensing applications [14]. We demonstrate complete filling of such a dry-etched angled-sidewall slot structure with titanium dioxide grown by the atomic layer deposition technique. The effect of sidewall angle on slot filling with conformal growth methods is discussed.

Angled sidewalls also affect the mode confinement properties of the waveguide, which has been briefly discussed in earlier studies [15, 16]. However, the comparisons have been made between slot waveguides with different cross sectional area, and it is therefore difficult to observe the fact that the angled sidewalls actually enhance the vertical confinement of the optical field [14, 17]. In this work, we study the optical confinement with different sidewall angles, having our emphasis on materials that can be grown by ALD. We also study the effect of the sidewall angle and filling material on the nonlinear properties of the waveguides.

2. Slot filling with atomic layer deposition

The improved accessibility from top in the angled-sidewall slot waveguides can be utilized in filling them with a conformal growth method such as ALD. Whereas filling a straight-sidewall slot yields a narrowed slot with its aspect ratio approaching infinite, an angled slot presents an easily fillable V-shaped structure. The difference is schematically depicted in Fig. 1. The following growth tests show that angled-wall slots can be conveniently filled with atomic layer deposition.

Figure 2 shows slot test structures fabricated on silicon substrates, and filled with ALD grown oxides. In Fig. 2(a), a 100 nm thick ALD grown layer of amorphous titanium dioxide (TiO_2) has been grown onto a slot test structure made by e-beam lithography and reactive ion etching. The precursors used in the growth are TiCl_4 and H_2O , and the growth temperature was 120 °C.

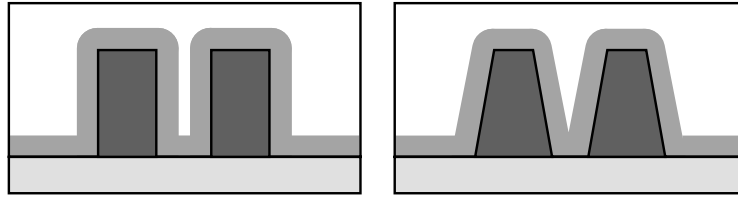


Fig. 1. Schematic comparison between an angled and a straight slot when filled with conformal growth.

Figure 2(a) shows that the slots are completely filled. Titanium dioxide is one of the most common ALD grown materials, and it is also a promising candidate for an ALD grown nonlinear slot filling material. It has a refractive index of 2.2. Moreover, it has been reported to exhibit a very large nonlinear index n_2 for an oxide; it is about 50 times larger than n_2 of silica [18]. Using prism coupling measurements, optical loss of the ALD grown titanium dioxide has been observed to be less than 1 dB/cm [19], which is several times smaller than the typical loss in the slot waveguide itself. The literature value for n_2 is for TiO_2 bulk single crystal. Therefore, n_2 for an amorphous thin film may differ. Nevertheless, the literature value and our experiment show that titanium dioxide is a very promising ALD grown filling material for nonlinear photonic devices.

In Figure 2(b), another slot test structure has been filled with a laminate, which consists of alternating 10 nm layers of titanium dioxide and aluminum oxide. The refractive index of aluminum oxide is 1.64; note that by varying the layer thicknesses, the Al_2O_3 - TiO_2 laminate therefore enables any refractive index between 1.64 and 2.2. Using ALD grown fluorides (CaF_2 or MgF_2), refractive index as low as 1.36 is possible [13].

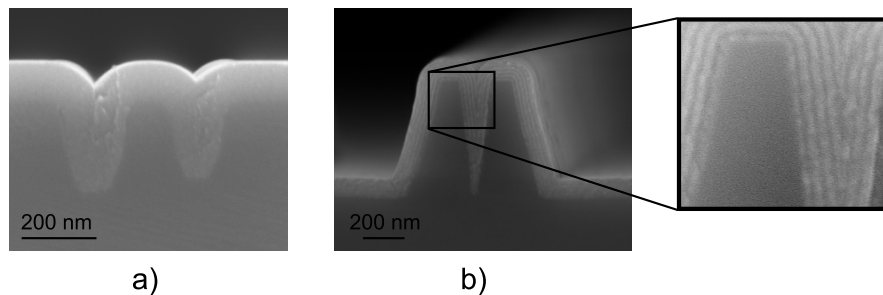


Fig. 2. Scanning electron micrograph of a cross section of slot waveguide test structures filled with a) ALD grown titanium dioxide, b) laminate of alternating layers of aluminum oxide and titanium oxide.

Table 1 summarizes material parameters of the most typical oxides and some nonlinear slot waveguide filling materials proposed in other studies. For some materials, references do not give exact values for nonlinearity; instead, ranges for nonlinear refractive index are given. We chose values close to the middle of their variation range so that $n_2(\text{TiO}_2)=50 \cdot n_2(\text{SiO}_2)$ and $n_2(\text{Si})=200 \cdot n_2(\text{SiO}_2)$. Nonlinear loss is assumed to be negligible for materials having bandgap twice as large as photon energy at $1.55 \mu\text{m}$ (i.e., $E_g > 1.6 \text{ eV}$).

Some polymers exhibit high optical nonlinearities [20–23], and ALD growth of polymers (polyimides) has been demonstrated [24]. Silica-embedded silicon nanocrystals are a well-known nanocomposite, whose nonlinearity can be orders of magnitude higher than that of its base materials. The nanolaminate in Fig. 2(b) suggests that ALD can also be a very versatile

tool in growing nanocomposites. Silicon nanocrystals can also be ion implanted into other host materials, which can be grown e.g. with ALD.

Table 1. Material parameters used in the calculations, and the wavelengths for the given parameters. (*)Ref. [26] gives values for $\lambda=1 \mu\text{m}$ and for $\lambda \rightarrow \infty$.

Material	n	n_2 [m^2/W]	$\frac{n_2}{n_2(\text{SiO}_2)}$	α_2 [m/W]	ref.	λ [μm]
SiO ₂	1.44	$3.2 \cdot 10^{-20}$	1	0	[25]	1.55
Si	3.48	$6.4 \cdot 10^{-18}$	200	$4.5 \cdot 10^{-11}$	[20]	1.55
TiO ₂	2.2	$1.6 \cdot 10^{-18}$	50	0	[18,26]	1.064, (*)
Al ₂ O ₃	1.64	$2.8 \cdot 10^{-20}$	0.875	0	[18,27]	1.064, 1.55
PMDA-PDA	1.5	$\approx 10^{-18}$	32	0	[23]	1.907
DDMEBT	1.8	$1.6 \cdot 10^{-17}$	500	0	[21,22]	1.55
Si nc 8 at. %	1.55	$9.5 \cdot 10^{-17}$	3000	$2 \cdot 10^{-10}$	[7,28]	1.55
Si nc 20 at. %	1.81	$8 \cdot 10^{-17}$	2500	$1 \cdot 10^{-10}$	[7,28]	1.55

In the following, we will study the effect of the sidewall angle and the filling material on the mode confinement in the slot waveguides. Finally, we will calculate figures of merit for ALD filled slot waveguides in all-optical devices.

3. Modefields in angled-sidewall slot waveguides

The considered waveguide is a thin-film-filled silicon slot waveguide, whose schematic with its parameters is shown in Fig. 3. Such a slot waveguide is fabricated by etching the pattern of two rails (width w_r) into a SOI substrate with a top silicon layer thickness h [5], and covering the structure with a thin film of a thickness t_c . The width of the angled slot between the rails is defined by the bottom and center widths w_{sb} and w_s , respectively. All the sidewalls of the rails are assumed to have the same sidewall angle, as shown in Fig. 3.

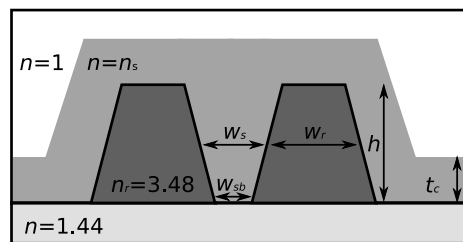


Fig. 3. Schematic of the thin-film-filled slot waveguide and introduction of its parameters.

Figures 4(a) and 4(b) show the mode intensity distribution in a SiO₂ filled slot waveguide with $n_s=1.44$, $w_s=80 \text{ nm}$, $w_r=160 \text{ nm}$ and $h = 260 \text{ nm}$ for two different bottom widths. The simulations in this work are carried out for the quasi-TE mode at the wavelength of $1.55 \mu\text{m}$, using the finite element solver of the FimmWave software [29].

With $w_{sb} < w_s$, the modefield is concentrated more to the bottom of the slot. This phenomenon can be explained with the higher average refractive index at the region with the larger rail width and smaller slot width [14, 30]. The modefields in a TiO₂ filled slot (i.e., $n_s=2.2$), shown in Figs. 4(c) and 4(d), do not show as evident vertical field compression. This is due to the smaller contrast between the rail and filling materials.

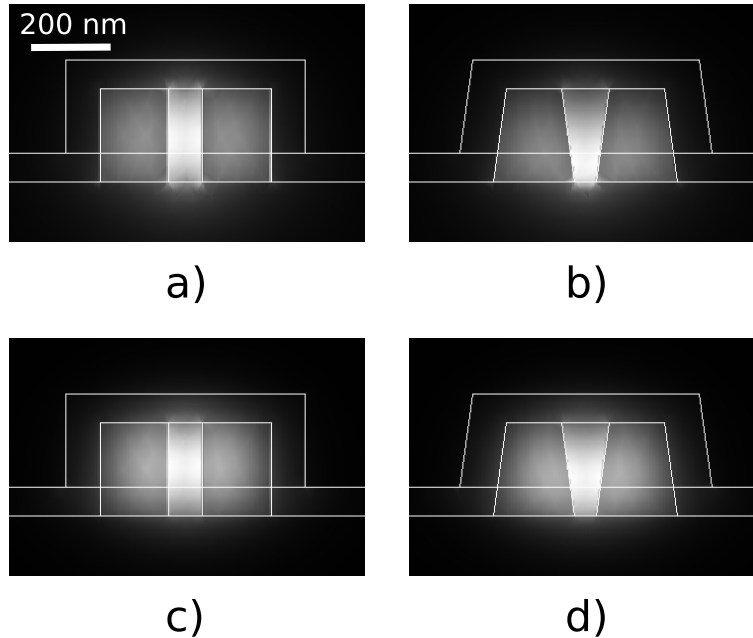


Fig. 4. Mode intensity distribution in a slot waveguide with $n_s=1.44$, $w_s=80$ nm, $w_r=160$ nm and $h = 260$ nm and a) $n_s=1.44$ and $w_{sb}=80$ nm, b) $n_s=1.44$ and $w_{sb}=50$ nm, c) $n_s=2.2$ and $w_{sb}=80$ nm, d) $n_s=2.2$ and $w_{sb}=50$ nm.

Figure 5 shows the effective mode area [20]

$$A_{\text{eff}} = \frac{Z_0^2 \left| \int \text{Re} \{ E(x,y) \times H^*(x,y) \} \cdot \mathbf{u}_z dA \right|^2}{n^2 \int |E(x,y)|^4 dA} \quad (1)$$

in a slot waveguide with $w_s=80$ nm, $w_r=160$ nm and $h = 260$ nm, as a function of w_{sb} , with several suggested slot filling materials. In Eq. (1), E and H are the electric and magnetic fields, respectively, Z_0 is the impedance of vacuum (377Ω), n is the refractive index of the (filling) material, and \mathbf{u}_z is the unit vector into the propagation direction.

The integrations in Eq. (1) are performed over the whole mode area. In order to be able to compare the confinement phenomenon with different filling materials, we do not take into account nonlinearities of different materials at this point; this question is analyzed later in this study. Note that using the geometry parameters chosen as shown in Fig. 3, the area of the slot cross section remains unchanged when varying w_{sb} . Therefore, these choices make it straightforward to study the effect of the sidewall angle on the optical confinement property of the waveguide.

With $n_s \leq 1.44$, the effective area decreases when decreasing w_{sb} . The effective area is constant between $w_{sb}=80$ nm and $w_{sb}=70$ nm and it decreases fastest with $w_{sb} < 60$ nm. Nevertheless, the effect can be seen with any w_{sb} of less than 70 nm.

As expected from the difference between Figs. 4 (b) and 4(d), the effective area is less affected by the sidewall angle with higher refractive index values for the filling material. With $n_s = 2.2$, the effective area in fact increases slightly with decreasing w_{sb} . When the index contrast between the rail and filling materials is lower, the vertical gradient in the average refractive index in the structure is smaller and the vertical confinement is less pronounced.

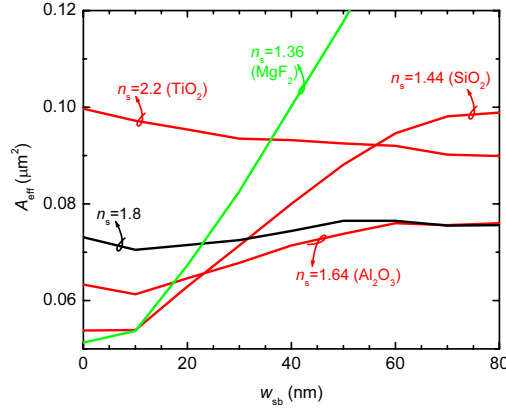


Fig. 5. Effective mode area in a slot waveguide with $w_s=80$ nm, $w_T=160$ nm and $h = 260$ nm, as a function of w_{sb} , with cover materials of different refractive indices.

4. Figures of merit for all-optical devices

In order to evaluate the expected performance of real all-optical devices, nonlinearities in each part of the waveguide need to be taken into account. We calculate the effective nonlinearity of the mode as

$$\gamma = \frac{n^2}{Z_0^2} \frac{\int |E(x,y)|^4 \cdot n_2(x,y) dA}{|\int \text{Re} \{E(x,y) \times H^*(x,y)\} \cdot \mathbf{u}_z dA|^2}, \quad (2)$$

which gives the effective index change of the waveguide mode caused by the optical power in units $1/W$. In silicon based all-optical devices, the nonlinear loss parameter α_2 is of an essential importance. In order to determine a figure of merit for the nonlinear index change against nonlinear loss in the waveguide, we carry out a calculation of the ratio between of these two:

$$\text{FOM}_{n_2/\alpha_2} = \frac{\int |E(x,y)|^4 \cdot n_2(x,y) dA}{\int |E(x,y)|^4 \cdot \alpha_2(x,y) dA}. \quad (3)$$

Note that even when the filling material is assumed to exhibit no nonlinear loss, some nonlinear loss exists in the waveguide, because a small fraction of the electric field resides in the silicon rails with a considerable nonlinear loss. The refractive index values and nonlinear parameters used in calculations are shown in Table 1.

4.1. Nonlinear devices

Figure 6 shows the effective nonlinearity and $\text{FOM}_{n_2/\alpha_2}$ in TiO_2 filled slot waveguides as a function of w_{sb} and w_s . Note that for silicon, $\text{FOM}_{n_2/\alpha_2} = 1.42 \cdot 10^{-7}$ m. It has also been plotted into Fig. 6 to give a reference for the performance of silicon waveguides.

The effective nonlinearity is not much affected by the sidewall angle, indicating that the vertical mode compression is not very significant with titanium oxide ($n = 2.2$) as the cover material. The n_2/α_2 figure of merit decreases with increasing sidewall angle. The decrease of $\text{FOM}_{n_2/\alpha_2}$ indicates weakened mode confinement of the mode into the slot: with a larger fraction of the optical field in silicon, the mode experiences a higher nonlinear loss.

Despite being highly nonlinear for an oxide, titanium dioxide still has a lower nonlinearity than silicon. Therefore, materials with higher nonlinearity would be desired to realize extremely nonlinear slot waveguide. Nonlinear polymers with even higher nonlinearity than silicon have

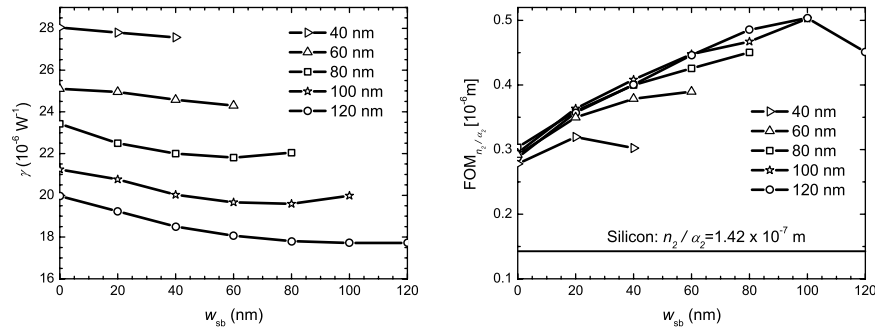


Fig. 6. Effective nonlinearity and n_2/α_2 figure of merit in TiO_2 filled slot waveguides with $w_T=160$ nm and $h = 260$ nm, as a function of w_{sb} at different w_S from 40 nm to 120 nm.

been demonstrated [21]. The calculated effective area and $\text{FOM}_{n_2/\alpha_2}$ in DDMEBT filled slot waveguides is shown in Fig. 7. The effective nonlinearity is about 10 times higher than in TiO_2 filled slot waveguides. With refractive index of 1.8, the angled sidewalls do not have significant effect on the nonlinearity. Similarly to the titanium dioxide filled waveguide, the $\text{FOM}_{n_2/\alpha_2}$ drops with increasing the sidewall angle. The n_2/α_2 figure of merit is up to 20 times higher than with TiO_2 filling. The improvement arises not only from the higher nonlinearity of DDMEBT, but also from its smaller refractive index, which yields improved field confinement to the slot.

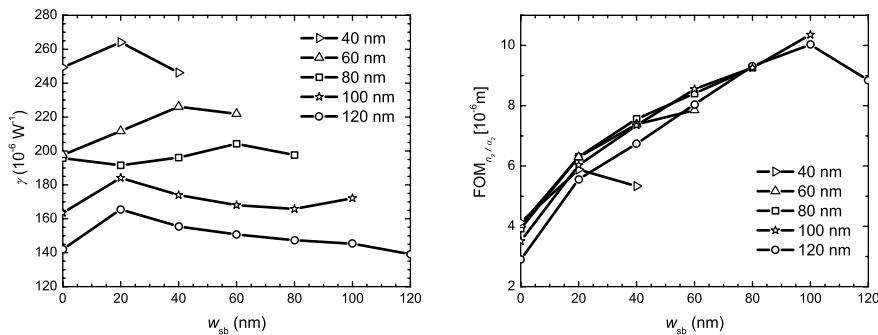


Fig. 7. Effective nonlinearity, and n_2/α_2 figure of merit as a function of w_{sb} in slot waveguides filled with DDMEBT polymer at different w_S from 40 to 120 nm, having geometry parameters $w_T=160$ nm and $h = 260$ nm.

Even though excellent nonlinear properties have been demonstrated with polymer-clad silicon slot waveguides, inorganic materials have benefits over polymers in terms of manufacturability and environmental stability. One example of an inorganic highly nonlinear material is silicon nanocrystals, which are reported to have nonlinearity of nearly 100 times larger than TiO_2 . The refractive index of such a material system can be as low as 1.55 [7, 28]. Therefore, angled sidewalls have advantages with this material system, as seen in Fig. 8. The effective nonlinearity for Si nanocrystal filled slot waveguides is about 50 times larger than with TiO_2 , and it increases significantly with angled sidewalls. Note that the n_2/α_2 figure of merit for silicon nanocrystals is $8 \cdot 10^{-7}$ m, and for silicon it is $1.42 \cdot 10^{-7}$ m. The nonlinear loss of silicon

nanocrystal filled silicon slot waveguides is therefore limited by FOM_{n_2/α_2} of silicon nanocrystals. It can be seen that with nearly vertical sidewalls, FOM_{n_2/α_2} of silicon nanocrystal filled slot waveguides is very close to that of silicon nanocrystal material, indicating strong optical confinement into the slot. FOM_{n_2/α_2} decreases slightly when $w_{sb} = 0$, due to a larger fraction of the field in the silicon rails when w_{sb} is small.

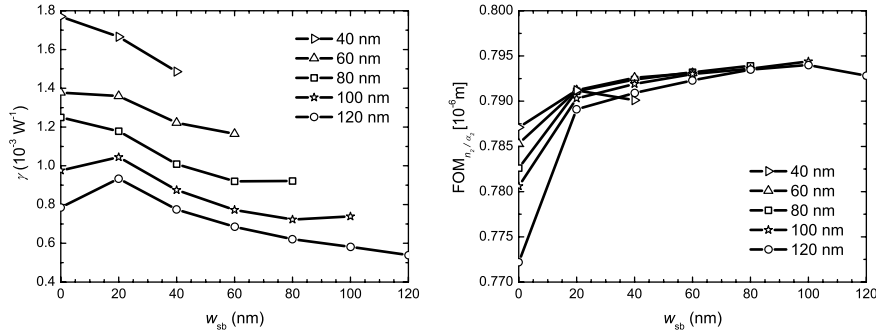


Fig. 8. Effective nonlinearity and FOM_{n_2/α_2} in silicon nanocrystal filled slot waveguides with $w_r=160$ nm and $h = 260$ nm, as a function of w_{sb} at different w_s from 40 nm to 120 nm.

Silicon nanocrystals are an example of a nanocomposite, which might provide several orders of magnitude higher nonlinearity than SiO_2 [15]. Figure 2(b) shows a promising example of ALD growth of a nanocomposite. Therefore, ALD might provide a very powerful tool to grow highly nonlinear nanocomposites in a very controlled and mass-producible way. The ultimate precision of ALD growth might even make it possible to engineer such a nanocomposite to exhibit maximal nonlinearity.

4.2. Filling with Al_2O_3

Aluminum oxide is one of the most common ALD materials. It is also a very common material for Er doped waveguide amplifiers [31]. ALD has been proven to be suitable for growing materials with well-controlled doping [32]; therefore, ALD filled slot waveguides are a very potential candidate if one considers silicon based emitters for telecommunication wavelengths.

The modal gain in a high-index-contrast waveguide can be calculated using the confinement factor Γ , which gives the ratio of the modal gain in the waveguide to the bulk gain of the filling material [33]

$$\Gamma = \frac{n_{AC}\epsilon_0 \int_{GM} |E(x,y)|^2 dA}{\int \text{Re} \{E(x,y) \times H^*(x,y)\} \cdot \mathbf{u}_z dA}, \quad (4)$$

where the integration in the numerator is carried out for the gain material (i.e., Al_2O_3). Figure 9 shows the confinement factor in an Al_2O_3 filled slot waveguide. The confinement factor decreases at small w_{sb} . With a larger sidewall angle, a larger fraction of light resides in the silicon rails near the bottom of the slot, and even though the vertical confinement is slightly enhanced (Fig. 5), the confinement factor decreases. However, the confinement factor is not much affected by the angled sidewalls at slot bottom width of 40 nm or more.

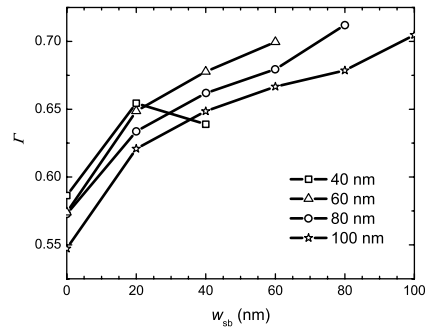


Fig. 9. Confinement factor for gain in Al_2O_3 filled slot waveguides with $w_r=160$ nm and $h = 260$ nm, as a function of w_{sb} at different w_s from 40 nm to 100 nm.

5. Discussion

The vertical confinement is enhanced with angled sidewalls, because the field maximum moves toward the region where the rails are wider and the slot narrower. This phenomenon reduces the effective area of the mode, enabling e.g. nonlinear functions with smaller optical power. The effect is observed with filling materials having a refractive index of 1.8 or smaller. Mode confinement toward the bottom of the slot may also reduce the amount of cover material needed to be grown.

On the other hand, small sidewall angles, which yield a slot width variation of less than 20 nm, do not usually have significant effect on the mode confinement. This might relax process requirements when aiming for slot waveguides with straight sidewalls: perfect verticality of the etching profile is not necessarily critical.

Titanium dioxide has a very high nonlinearity for an oxide, and TiO_2 filled slot waveguides were shown to exhibit potentially three times better performance than silicon strip waveguides, when comparing nonlinear index divided by nonlinear loss. Angled sidewalls were found to reduce the confinement factor to the filling material, which introduces increased nonlinear loss. Therefore, when aiming for e.g. titanium dioxide filled slot waveguides for nonlinear applications, straight or nearly straight sidewalls work best. ALD growth may work well in filling such slots as well; in order to ensure voidless filling, the most important task is to avoid a profile where slots are wider at the bottom. Such a slot would be closed from the narrowest point during the conformal growth, leaving void beneath.

6. Conclusion

The effect of angled sidewalls on the vertical mode confinement and conformal filling of slot waveguides was studied. Sidewall angles typical of reactive ion etching can have an enhancing effect on the effective area and nonlinearity of mode in slot waveguides. On the other hand, with larger sidewall angles, a larger fraction of optical power resides in the silicon rails, increasing nonlinear loss. Therefore, for optimum slot waveguide structure, proper balance between these effects needs to be found, depending on the used nonlinear slot material.

We demonstrated complete filling of slot waveguide structures with atomic layer deposited titanium dioxide films and with an $\text{Al}_2\text{O}_3/\text{TiO}_2$ laminates. The films appear to be completely free of voids, and ALD enables uniform growth over large areas.

The demonstrated growth of a nanolaminate also gives new possibilities to engineer slot

filling materials. The average refractive index inside the slot can be tuned by changing the layer thicknesses in the laminate. The $\text{Al}_2\text{O}_3/\text{TiO}_2$ laminate demonstrated in this work allows for adjusting the average refractive index in the range between 1.64 and 2.2. ALD grown fluorides may enable even smaller refractive index. The nanolaminate also shows that ALD may have potential to be used in the manufacture of highly nonlinear nanocomposites with excellent precision.

Acknowledgments

TEKES, the Academy of Finland (grant 128827), and Ministry of Education (The Research and Development Project on Nanophotonics) are acknowledged for financial support.